Old Dominion University
ODU Digital Commons

Electrical & Computer Engineering Faculty Publications | Electrical & Computer Engineering

2012

Optical Detection of Melting Point Depression For Silver Nanoparticles Via In Situ Real Time Spectroscopic Ellipsometry

S. A. Little

T. Begou
Old Dominion University

R. W. Collins

S. Marsillac
Old Dominion University, Smarsill@odu.edu

Follow this and additional works at: https://digitalcommons.odu.edu/ece_fac_pubs

 Part of the Engineering Science and Materials Commons, and the Optics Commons

Repository Citation

Little, S. A.; Begou, T.; Collins, R. W.; and Marsillac, S., "Optical Detection of Melting Point Depression For Silver Nanoparticles Via In Situ Real Time Spectroscopic Ellipsometry" (2012). *Electrical & Computer Engineering Faculty Publications*. 7.
https://digitalcommons.odu.edu/ece_fac_pubs/7

Original Publication Citation

Little, S.A., Begou, T., Collins, R.W., & Marsillac, S. (2012). Optical detection of melting point depression for silver nanoparticles via in situ real time spectroscopic ellipsometry. *Applied Physics Letters, 100*(051107), 1-3. doi: 10.1063/1.3681367

This Article is brought to you for free and open access by the Electrical & Computer Engineering at ODU Digital Commons. It has been accepted for inclusion in Electrical & Computer Engineering Faculty Publications by an authorized administrator of ODU Digital Commons. For more information, please contact digitalcommons@odu.edu.

AIP | Applied Physics Letters

Optical detection of melting point depression for silver nanoparticles via in situ real time spectroscopic ellipsometry

S. A. Little, T. Begou, R. W. Collins, and S. Marsillac

Citation: Applied Physics Letters **100**, 051107 (2012); doi: 10.1063/1.3681367
View online: http://dx.doi.org/10.1063/1.3681367
View Table of Contents: http://scitation.aip.org/content/aip/journal/apl/100/5?ver=pdfcov
Published by the AIP Publishing

Articles you may be interested in

Determination of the optical properties and size dispersion of Si nanoparticles within a dielectric matrix by spectroscopic ellipsometry
J. Appl. Phys. **116**, 103520 (2014); 10.1063/1.4894619

Evolution of optical properties of tin film from solid to liquid studied by spectroscopic ellipsometry and ab initio calculation
Appl. Phys. Lett. **104**, 121907 (2014); 10.1063/1.4869722

Growth analysis of (Ag,Cu)InSe2 thin films via real time spectroscopic ellipsometry
Appl. Phys. Lett. **101**, 231910 (2012); 10.1063/1.4769902

Analysis of interband, intraband, and plasmon polariton transitions in silver nanoparticle films via in situ real-time spectroscopic ellipsometry
Appl. Phys. Lett. **98**, 101910 (2011); 10.1063/1.3564894

Real-time spectroscopic ellipsometry study of Ta–Si–N ultrathin diffusion barriers
J. Vac. Sci. Technol. A **23**, 1359 (2005); 10.1116/1.1996612

This article is copyrighted as indicated in the article. Reuse of AIP content is subject to the terms at: http://scitation.aip.org/termsconditions. Downloaded to IP: 128.82.253.83 On: Fri, 08 Jan 2016 00:46:17

Optical detection of melting point depression for silver nanoparticles via *in situ* real time spectroscopic ellipsometry

S. A. Little,[1] T. Begou,[2] R. W. Collins,[1] and S. Marsillac[2,a)]
[1]*Center for Photovoltaics Innovation and Commercialization (PVIC), University of Toledo, Toledo, Ohio 43606, USA*
[2]*Department of Electrical and Computer Engineering, Old Dominion University, Norfolk, Virginia 23529, USA*

(Received 12 November 2011; accepted 13 January 2012; published online 1 February 2012)

Silver nanoparticle films were deposited by sputtering at room temperature and were annealed while monitoring by real time spectroscopic ellipsometry (SE). The nanoparticle dielectric functions (0.75 eV–6.5 eV) obtained by SE were modeled using Lorentz and generalized oscillators for the nanoparticle plasmon polariton (NPP) and interband transitions, respectively. The nanoparticle melting point could be identified from variations in the oscillator parameters during annealing, and this identification was further confirmed after cooling through significant, irreversible changes in these parameters relative to the as-deposited film. The variation in melting point with physical thickness, and thus average nanoparticle diameter, as measured by SE enables calculation of the surface energy density. © *2012 American Institute of Physics*. [doi:10.1063/1.3681367]

In situ control of the structural, thermal, electrical, and optical properties of metallic nanoparticles via surface engineering is motivated by their many applications.[1] The varied applications of silver in nanoparticle form include low temperature interconnects, nanoantennas, sensors for biological materials, and back contact reflectors in thin film solar cells. *In situ* control is enabled through thin film processing, as well as through thermal annealing of the resulting nanoparticle films, in conjunction with non-invasive *in situ* measurement techniques. For example, deposition or annealing at elevated temperatures shapes nanoantennas and incorporates surface structure into back reflectors for optical enhancement in photovoltaics.[1] In research described in the present article, Ag films—incorporating isolated nanoparticles and having a range of thickness—were deposited at room temperature and then annealed at temperatures up to 773 K while analyzing *in situ* by real time spectroscopic ellipsometry (SE).

The Ag nanoparticle films were deposited by dc magnetron sputtering at 288 K onto Si (100) wafers with 500 nm thermal oxides.[1] The deposition times were varied from 0.5 to 3 min, which led to films of increasing thicknesses characterized by an array of isolated nanoparticles of average size increasing from 2 nm to 10 nm, respectively.[1,2] To determine the dielectric functions of these films, a rotating-compensator multichannel ellipsometer was used having a photon energy range of 0.75–6.50 eV. Pairs of (ψ, Δ) spectra were collected with a 65° incidence angle and a 3 s acquisition time. These spectra were modeled assuming one or two substrate-supported layers, applying the effective medium theory and dielectric function analytical form given previously.[1] *Ex situ* measurements including atomic force microscopy (AFM), x-ray diffraction (XRD), scanning electron microscopy (SEM), and secondary ion mass spectrometry (SIMS) were used to complement as well as corroborate the real time SE results. Temperature measurements of the Ag thin films were obtained in accordance with a previously described technique.[2]

For generality in fitting (ψ, Δ) data by least-squares regression, the starting structural model consists of two layers, a coalesced or "bulk" layer and a surface roughness layer, with thicknesses d_b and d_s, respectively, incorporated as free parameters. The following analytical form for the dielectric function of the nanoparticles was used:[1]

$$\varepsilon(E) = \varepsilon_\infty + \frac{A_L^2}{E_L^2 - E^2 - i\Gamma_L E} + G(E), \tag{1}$$

where

$$G(E) = A_G(\Gamma_G/2)^{-\mu}\left\{e^{i\phi}[E_G - E - i(\Gamma_G/2)]^\mu + e^{-i\phi}[E_G + E + i(\Gamma_G/2)]^\mu\right\}. \tag{2}$$

The first term in Eq. (1) describes an offset; the second term describes a Lorentz oscillator for the nanoparticle plasmon polariton (NPP) with amplitude A_L, resonance energy E_L, and broadening Γ_L; the third term describes the interband transition with amplitude A_G, band gap energy E_G, broadening Γ_G, phase ϕ, and exponent μ.

The dominant nanoparticle nature of the deposited films was evidenced by the need for the Lorentz oscillator in the dielectric function model. The oscillator resonance energy E_L is observed to redshift with increasing thickness and thus particle size, consistent with increasing dipole-dipole interactions between particles.[3] Because no Drude component was needed to fit the dielectric functions and because d_b remained below a single monolayer in a two-layer analysis, it could be verified that all depositions were terminated prior to coalescence, with the resulting films consisting of *isolated* nanoparticles. This was further corroborated by *ex situ* SEM and AFM images obtained immediately after selected depositions, as depicted in Fig. 2.

a)Author to whom correspondence should be addressed. Electronic mail: smarsill@odu.edu.

 © 2012 American Institute of Physics

This article is copyrighted as indicated in the article. Reuse of AIP content is subject to the terms at: http://scitation.aip.org/termsconditions. Downloaded to IP: 128.82.253.83 On: Fri, 08 Jan 2016 00:46:17

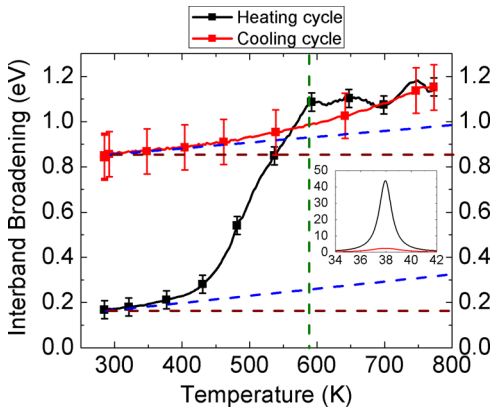

FIG. 1. (Color online) Interband broadening parameter as a function of temperature for nanoparticles in a Ag film with $d_s = 8.42$ nm. The vertical line is guide to the eye for the transition point and the broken lines are variations predicted on the basis of electron-phonon interactions alone. Inset: XRD spectra of the Ag (111) peak before (upper curve) and after (lower curve) the thermal cycle (vertical axis, intensity in arbitrary units; horizontal axis, angle 2θ in degrees).

After characterization of the as-deposited nanoparticle film, its SE data were acquired *in situ* and in real time during annealing from 288 K to 773 K and then during cooling to 288 K. The continuous temperature (T) evolution of the interband broadening parameter Γ_G, deduced by SE, is shown in Fig. 1 for a nanoparticle film with $d_b = 0$ nm, $d_s = 8.42$ nm. An increase in T can lead to an increase in Γ_G simply due to the increased electron-phonon interactions at higher T.[4] This effect is described by the broken lines in Fig. 1, most accurately determined in the later stages of cooling when structural changes due to annealing are minimized.

The most obvious feature in Fig. 1, however, is the abrupt change in the evolution of Γ_G at $T \sim 595$ K. This is attributed to the melting transition associated with the largest particles of the film which define its physical thickness d_s.[5] During annealing, the broadening that occurs above the broken line dependences in Fig. 1 must be due to structural changes in the nanoparticle film. For $400 < T < 595$ K, during annealing the excess broadening may be due to melting of the smallest particles which occur at reduced T. For $500 < T < 595$ K, during cooling the excess broadening may have a similar origin—liquid particles that recrystallize over a range of T due to the distribution of particle sizes. Broadening may also occur upon heating and cooling due to strain-induced lattice deformation.[5]

The parameters for representative dielectric functions are reported Table I for nanoparticles in a film with an as-deposited thickness of $d_s = 6.48$ nm (i) at 288 K in the as deposited state, (ii) at 773 K during annealing, and (iii) at 288 K after annealing. The MSE data given in Table I are in accordance with other references.[6] Quantitative comparisons of these parameters yield several insights.

Upon heating to 773 K, significant increases occur not only in Γ_G (0.18 to 1.11 eV), as indicated in Fig. 1, but also in Γ_L, the broadening parameter of the NPP resonance (0.83 to 3.57 eV).[7,8] This consistent behavior in both interband and NPP transitions is attributed to a loss of long range order due to melting which occurs at 595 K and leads to an electron mean free path λ on the order of the atomic spacing. Applying an estimate of $\lambda = \hbar v_F/\Gamma_L$ for the free electrons of the NPP band, where $v_F \sim 1.4 \times 10^8$ cm/s is the bulk Fermi velocity and $\hbar$ is Planck's constant, values of Γ_L of 0.83 and 3.57 eV correspond to λ values of 1 nm, approximately one-third the particle radius, and 0.25 nm, approximately the atomic spacing, respectively. Cooling to room temperature leads to only a partial recovery of the broadening parameters (interband: 1.11 to 0.82 eV; NPP: 3.57 to 2.17 eV). Recrystallization to a more defective crystalline or a disordered nanocrystalline structure relative to the as-deposited structure is responsible for this behavior,[5] a surprising observation that will be discussed in further detail below.

In addition in Table I, a significant decrease in A_L, the NPP amplitude, is noted (from 15.5 to 0.5 eV). This behavior is attributed primarily to the broadening of the interband transition which gives rise to a larger ε_2 value at the NPP energy and hence a suppression of the resonance. An unaccounted for increase in void fraction f_v in the film may also occur during heating due to nanoparticle coarsening, which leads to an increase in d_s, at constant effective thickness (defined as $d_{\text{eff}} = f_v\, d_s$ or the volume of particles per area). The latter effect is likely to be reflected clearly in the reduction in A_G, the interband amplitude upon annealing. Cooling to room temperature again leads to only a partial recovery of the NPP amplitude (0.5 to 0.9 eV), consistent with the sharpening of the interband component and a reduction in ε_2 at the NPP resonance. The interband amplitude continues to decrease consistently which could result from nanoparticle coarsening during cooling; however, a contribution may also exist due to lattice deformation, as was suggested by XRD with the lowering and broadening of the Ag (111) peak. The reduction of the interband amplitude term also contributed to the increased uncertainty of the interband broadening (Fig. 1) by effectively reducing the signal-to-noise ratio for this oscillator and thus also contributes to the increase in MSE tabulated in Table I.

For E_L, the NPP resonance energy, a blue shift upon annealing from 2.68 to 3.21 eV indicates a decrease in dipole-dipole interactions due to the weaker NPP resonance and the larger spacing between particles[3] as indicated in the Fig. 2. The partial red shift upon cooling is consistent with the accompanying increase in the resonance amplitude. For E_G, the interband energy onset, various competing effects can occur. An increase in temperature leads to a decrease in interband energy due to the electron-phonon interaction, by $\sim$0.1 eV over the temperature range of 288 K to 595 K.[4] Annealing can also induce lattice deformation and particle size changes which can also change the band gap due to strain and size effects.[5] The reduction in E_G at room temperature by the heating-melting-cooling cycle may be attributable to the increase in nanoparticle size as shown in Fig. 2.

A key focus of this research is characterization of the melting point depression for the nanoparticles—in the case of Fig. 1 from 1235 K to 595 K for a film with $d_s = 8.42$ nm.[4] This depression is due to the high surface to volume ratio and the lower cohesive energy of surface atoms. The melting point is thus a function of the nanoparticle shape, radius, or any other structural parameters that can modify the surface to volume ratio. The melting point temperature can be described by the following equation:[7]

This article is copyrighted as indicated in the article. Reuse of AIP content is subject to the terms at: http://scitation.aip.org/termsconditions. Downloaded to IP: 128.82.253.83 On: Fri, 08 Jan 2016 00:46:17

TABLE I. The oscillator parameters that define the dielectric functions of the Ag nanoparticles at different stages in the thermal cycle. The physical thickness is 6.48 nm for the as-deposited film composed of isolated Ag nanoparticles.

	NPP			Interband		
Stage/MSE	A_L	Γ_L (eV)	E_L (eV)	A_G	Γ_G (eV)	E_G (eV)
285 K[a]/0.019	15.5 ± 0.9	0.83 ± 0.01	2.68 ± 0.01	4.1 ± 0.2	0.18 ± 0.03	4.34 ± 0.02
773 K/0.033	0.5 ± 0.1	3.57 ± 0.10	3.21 ± 0.04	3.2 ± 0.1	1.11 ± 0.04	4.51 ± 0.05
285 K[b]/0.024	0.9 ± 0.3	2.17 ± 0.52	3.01 ± 0.35	3.0 ± 0.2	0.82 ± 0.10	4.19 ± 0.15

[a]Room temperature before heating.
[b]Room temperature after heating.

$$T_m(d_s) = T_o - \frac{2T_o M\sigma_s}{\Delta H_o \rho_s} \cdot \frac{1}{1/2 d_s}, \quad (3)$$

where σ_s is the surface energy density and is used as a fitting parameter; T_o is the bulk melting point (1235 K); M is the molar mass of Ag (107.87 g/mol); ΔH_o is the enthalpy of melting (11.28 kJ/mol); ρ_s is the mass density of Ag (10.49 g/cm^3); and d_s is extracted from RTSE. In fact, d_s is assumed to be equal to the diameter of the largest particles in the distribution and, thus, dominates the melting behavior. A discussion of the effects of the particle density concerning similar films was reported previously.[3] In Fig. 3, the nanoparticle film melting point is shown, deduced from data similar to those of Fig. 1 and plotted as a function of $1/2 d_s$, or the estimated particle radius. Fitting the results in Fig. 3 using Eq. (3) leads to a surface free energy density of $\sigma_s = 0.9$ J/m^2, which is in reasonable agreement with previously reported values for both bulk Ag (1.0–1.5 J/m^2)[9] and substrate supported nanoparticles (1.1 J/m^2)[10] but much lower than values reported for free nanoparticles (~6.4–7.4 J/m^2).[9] The MSE values of individual fits were below 0.035, indicating a good fit.[6]

Ex-situ analyses were also performed to better understand the influence of the full annealing-melting-cooling cycle on the structure of the Ag nanoparticles. Both SEM and XRD results confirm the melting temperature of the nanoparticles through the significant differences in average size and crystallinity of particles before and after annealing cycles that reach the melting point.

By SEM, nanoparticles particles appeared larger and more uniform in size after an annealing cycle that exceeds the SE-deduced melting point, as shown in Fig. 2. Analysis by XRD, as depicted in the Fig. 1 inset, performed before heating reveals a characteristic Ag (111) peak, which nearly disappears after a full annealing-melting-cooling cycle, revealing that the bulk-like crystalline component of the nanoparticles has decreased. This result is likely to result from the increase in the volume of grain boundaries and other defective regions of the nanoparticles upon annealing—even to the extent that the nanoparticle material appears to exhibit an amorphous component. This structural change is consistent with significant broadening of the NPP and interband features measured after cooling, as seen in the analysis results of Table I. In fact, the increase in broadening of the NPP for the thermally cycled particles over the as-deposited particles can be attributed to decrease in mean free path from ~1 nm to 0.4 nm, the latter being much smaller than the observed particle size. The physical reason for the formation of defective particles after cooling from the liquid is unclear; cooling rates are too slow (4 K/min) to quench in such defects. One possibility is that such a structure is stabilized by surface adsorbates that are incorporated as impurities within the bulk nanoparticles upon melting. Secondary ion mass spectrometry has not detected differences between the contaminant levels before and after the annealing cycle; however, it is likely that nanoparticle impurities would be difficult to detect, given the presence of surface contamination in *ex situ* analyses.

In conclusion, sputter deposition of silver onto room temperature SiO_2 surfaces for increasing durations led to films consisting of isolated nanoparticles with increasing average sizes. The thin films were measured by real time SE during annealing and subsequent cooling, and the resulting

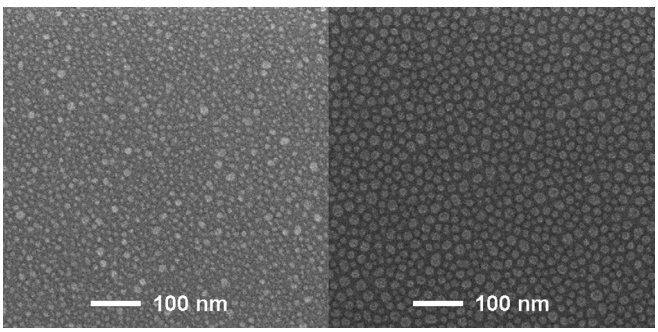

FIG. 2. SEM image (SEI mode) of a film as-deposited (left) and after the thermal cycle (right).

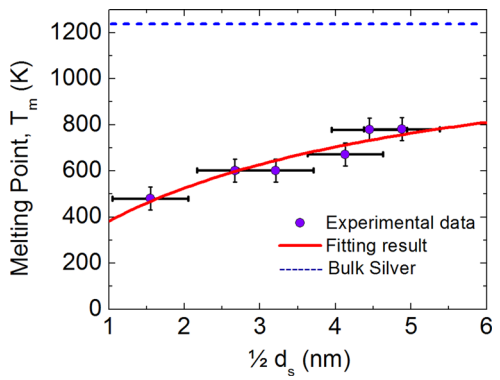

FIG. 3. (Color online) Melting point of silver nanoparticles plotted versus the average particle radius, estimated as one-half the physical thickness. The dashed line indicates the melting point of bulk silver. The solid line is the fit of Eq. (3), yielding the surface energy density.

This article is copyrighted as indicated in the article. Reuse of AIP content is subject to the terms at: http://scitation.aip.org/termsconditions. Downloaded to IP: 128.82.253.83 On: Fri, 08 Jan 2016 00:46:17

nanoparticle dielectric functions were modeled using parameterized oscillators. By observing the variations in the oscillator parameters upon annealing, at elevated temperature, and during cooling, key information on the nanoparticle structure and phase can be deduced. In particular, the broadening parameters of the NPP and interband transitions provide insights into electronic scattering and defects within the particles. A significant reduction in the free electron mean free path in nanoparticles identifies melting point depression, and partial recovery upon cooling indicates poorer crystallinity in the thermally cycled particles relative to the as-deposited particles. These conclusions based on non-invasive real time analysis were further confirmed by direct *ex situ* studies.

[1]S. A. Little, R. W. Collins, and S. Marsillac, Appl. Phys. Lett. **98**, 101910 (2011).
[2]A. R. Heyd, R. W. Collins, K. Vedam, S. S. Bose, and D. L. Miller, Appl. Phys. Lett. **60**, 2776 (1992).
[3]S. Marsillac, S. A. Little, and R. W. Collins, Thin Solid Films **519**, 2936 (2011).
[4]P. Winsemius, F. F. Van Kampen, H. P. Lengkeek, and G. G. Van Went, J. Phys. F: Met. Phys. **6**, 1583 (1976).
[5]D. Dalacu and L. Martinu, J. Appl. Phys. **87**, 228 (2000).
[6]B. Johs and C. M. Herzinger, Phys. Status Solidi C **5**, 1031 (2008).
[7]D. Dalacu and L. Martinu, Appl. Phys. Lett. **77**, 4283 (2000).
[8]M. Quaas, I. Shyjumon, R. Hippler, and H. Wulff, Z. Kristallogr. **26**(Suppl.), 267 (2007).
[9]K. K. Nanda, A. Maisels, F. E. Kruis, H. Fissan, and S. Stappert, Phys. Rev. Lett. **91**, 106102 (2003).
[10]T. Castro, R. Reifenberger, E. Choi, and R. P. Andres, Phys. Rev. B **42**, 8548 (1990).

This article is copyrighted as indicated in the article. Reuse of AIP content is subject to the terms at: http://scitation.aip.org/termsconditions. Downloaded to IP: 128.82.253.83 On: Fri, 08 Jan 2016 00:46:17